International Journal of Geo-Information

MDPI

*Article*

# Multistage Impacts of the Heavy Rain Process on the Travel Speeds of Urban Roads

**Qiuping Li [1,*], Haowen Luo [2] and Xuechen Luan [3]**

[1] School of Geography and Planning, Sun Yat-Sen University, Guangzhou 510275, China
[2] Department of Geography and Resource Management, The Chinese University of Hong Kong, Shatin, NT, Hong Kong 999077, China; haowen@link.cuhk.edu.hk
[3] Guangdong Fundway Science and Technology Corporation Limited, Guangzhou 510275, China; luanxch@mail.sysu.edu.cn
* Correspondence: liqp3@mail.sysu.edu.cn

**Abstract:** Heavy rain causes the highest drop in travel speeds compared with light and moderate rain because it can easily induce flooding on road surfaces, which can continue to hinder urban transportation even after the rainfall is over. However, very few studies have specialized in researching the multistage impacts of the heavy rain process on urban roads, and the cumulative effects of heavy rain in road networks are often overlooked. In this study, the heavy rain process is divided into three consecutive stages, i.e., prepeak, peak, and postpeak. The impact of heavy rain on a road is represented by a three-dimensional traffic speed change ratio vector. Then, the k-means clustering method is implemented to reveal the distinct patterns of speed change ratio vectors. Finally, the characteristics of the links in each cluster are analyzed. An empirical study of Shenzhen, China suggests that there are three major impact patterns in links. The differences among links associated with the three impact patterns are related to the road category, travel speeds in no rain days, and the number of transportation facilities. The findings in this research can contribute to a more in-depth understanding of the relationship between the heavy rain process and the travel speeds of urban roads and provide valuable information for traffic management and personal travel in heavy rain weather.

**Keywords:** heavy rain process; urban roads; traffic speeds; clustering analysis; taxi GPS data



**Citation:** Li, Q.; Luo, H.; Luan, X. Multistage Impacts of the Heavy Rain Process on the Travel Speeds of Urban Roads. *ISPRS Int. J. Geo-Inf.* **2021**, *10*, 557. https://doi.org/10.3390/ijgi10080557

Academic Editor: Wolfgang Kainz

Received: 6 May 2021
Accepted: 15 August 2021
Published: 17 August 2021



## 1. Introduction

Adverse weather conditions, such as rain, may significantly influence the traffic efficiency of urban roads, such as travel speeds and times, resulting in a deterioration of road network performance [1–6]. Heavy rain can cause the highest drop in travel speeds compared with light and moderate rain [5,7] because heavy rain can not only significantly reduce visibility but also induce flooding with a high probability, which increases accident risks and reduces roadway capacity [6,8–11]. Therefore, decision-makers should pay more attention to the impacts of the continuous heavy rain process on the traffic efficiency of urban roads when developing effective traffic management measures and enhancing city resilience to adverse weather.

Many studies have focused on the traffic performance deterioration of roads caused by rain. Much of the literature analyzes the average decrease in traffic efficiency, such as travel speeds and times, with different rainfall intensities [5,12–21]. The main related works are listed in Table 1. A general trend found in the literature of Table 1 is that the traffic efficiency decreases as rainfall intensity increases, although the extent of the decline varies. For instance, in the research of Agarwal et al. [15], the reduction in speeds on a freeway in Minneapolis was 1–2% (trace rain), 2–4% (light rain), and 4–7% (heavy rain). Tsapakis et al. [5] found that the ranges of the total travel time of some selected roads in London increased due to light, moderate, and heavy rain were the following: 0.1–2.1%,

1.5–3.8%, and 4.0–6.0%, respectively. On an urban road of Hong Kong, the reductions in travel speeds were approximately 4.21% under light rain conditions, 6.28% under medium rain conditions, and 7.31% under heavy rain conditions [18].

**Table 1.** Summary of selected research on the effect of rainy weather on traffic performance deterioration.

| Related Work | Year | Study Area | Road Type | Rainfall Intensity (mm/h) | Traffic Performance Deterioration | |
|---|---|---|---|---|---|---|
| Smith et al. [12] | 2004 | Virginia, United States | Freeway | Light<br>heavy | Reduction of capacity | 4–10%<br>25–30% |
| Agarwal et al. [15] | 2006 | Minneapolis, United States | Freeway | 0–0.26<br>0.26–6.35<br>>6.35 | Reduction of speed | 1–2%<br>2–4%<br>4–7% |
| Billot et al. [16] | 2009 | Paris, France | Freeway | 0–2<br>2–3 | Reduction of speed | 8%<br>12.6% |
| Tsapakis et al. [5] | 2013 | London, United Kingdom | Urban roads | 0–0.25<br>0.25–6.35<br>>6.35 | Increase of travel time | 0.1–2.1%<br>1.5–3.8%<br>4.0–6.0% |
| Lam et al. [18] | 2013 | Hong Kong, China | Urban roads | 0–0.5<br>0.5–6.5<br>>6.5 | Reduction of speed | 3.5–4.2%<br>5.7%<br>6.8–10.1% |
| Zhang et al. [20] | 2018 | Beijing, China | Urban roads | <2.4<br>8.0–16.0 | Reduction of speed | 3.0–4.7%<br>5.0–9.4% |
| Zhang et al. [21] | 2019 | Beijing, China | Urban Expressway | <2.4<br>2.4–6.0<br>>6.0 | Reduction of speed | 3.1%<br>5.3%<br>6.6% |

In addition to the traffic efficiency, the relationships of the traffic speed-flow-density were also affected by rainy weather. Much effort has been made to quantify the traffic speed-flow-density relationships on freeways and urban roads under rainy conditions [13,18,22,23]. For instance, Zhang et al. [23] calibrated the traffic speed-flow-density relationship based on the Van Aerde model [24] using real traffic and rainfall data of a freeway in Wuhan, China. Lam et al. [18] established a generalized traffic speed-flow-density relationship with varied rainfall intensities on a major section of an urban road of Hong Kong, and the calibrated speed-flow-density functions agree well with the observed data.

Moreover, some research found that the effects of rain on traffic efficiency vary with different road categories, locations, times, and congestion levels [5,11,20,25–28]. Andersen and Torp [23] examined rain's impact on four highways, two rural roads, and four urban roads and concluded that the decline in travel speeds was more pronounced on urban roads than on highways and rural roads. Tsapakis et al. [5] found that the highest increase in travel time was on the links located in outer London areas, whereas the smallest increase occurred in central London areas. Mitsakis et al. [11] divided their research area into several geographical zones and found that the impacts of rainfall varied considerably in each study zone. Qi et al. [27] found that the traffic flow on the roads within the urban inner space, such as the central business district (CBD), was more likely to be impacted by inclement weather compared with other suburbs. Yao et al. [28] indicated that road speeds decreased by 6.20% on weekdays and by 2.37% on weekends in rainfall weather. In addition, at different times of the day, the travel reliability during 0:00–2:00, 6:00–8:00, 12:00–14:00, and 22:00–24:00 was higher than those during other periods. Zhang et al. [20] derived a relationship between rainfall intensity and travel speed reduction for different congestion levels and found that light congestion was the most sensitive traffic condition to rainfall when there was moderate or heavier rain.

The abovementioned research provides a glimpse of the rich literature examining the impacts of rainfall on road traffic. However, very few studies have specialized in the multistage impacts of the heavy rain process on urban roads. Unlike light and moderate rain, continuous heavy rain can easily induce flooding on the road surface in its later stage [6,11]. The impacts on road traffic in the later stage would be higher than that in

the former stage, even if the rainfall intensities in these two periods are similar. These different impacts cannot be distinguished by previous works that simply examined the average traffic efficiency decrease under light, moderate and heavy rain conditions. Thus, it is necessary to differentiate the impacts of heavy rain on urban roads in various rainfall stages and consider the cumulative effects of the heavy rain process. A question that needs to be answered is: what are the typical impact patterns of the heavy rainfall process on the traffic speeds of urban roads?

In this study, we propose a multistage impact model that can reveal the effects of various heavy rain stages on the travel speeds of urban roads. In this model, the heavy rain process is divided into three consecutive stages: prepeak, peak, and postpeak. Then, the impacts of heavy rain on the travel speeds of a link in these three stages are represented by a three-dimensional travel speed variation vector. The k-means clustering method is implemented to classify these vectors into different clusters, and the main impact patterns are obtained. Finally, the spatial distribution and the characteristics of the links of each cluster are analyzed and compared.

The remainder of this paper is organized as follows. Section 2 introduces the study area and used data. Section 3 describes the methodology, including the multistage impact model of heavy rain on travel speeds and impact pattern discovery based on the k-means clustering method. The experimental results and analysis are presented in Section 4. The final section provides concluding remarks and future research directions.

## 2. Study Area and Data

### *2.1. Study Area*

The study area of this research is within the city of Shenzhen, China. Shenzhen is located in the Pearl River Delta, adjacent to the Hong Kong Special Administrative Region. The main climate type in Shenzhen is the subtropical monsoon climate with high temperature and humidity. The yearly cumulative rainfall of Shenzhen is approximately 2000 mm [29]. The spatial distribution of the rainfall is extremely uneven. The rainfall center is mainly located in central and southeastern Shenzhen, and the rainfall intensity decreases gradually from the center towards the surrounding areas. In this study, three districts of Shenzhen (Luohu, Nanshan, and Futian) were selected as the case study area (Figure 1) because they are central urban districts with rapid economic growth and highly developed transportation networks. The total number of links in this study is 2439. The numbers of links belonging to highways or urban expressways (HWUEs), arterial roads (ARs), collector roads (CRs), and other roads (ORs) are 165, 694, 1136, and 444, respectively.

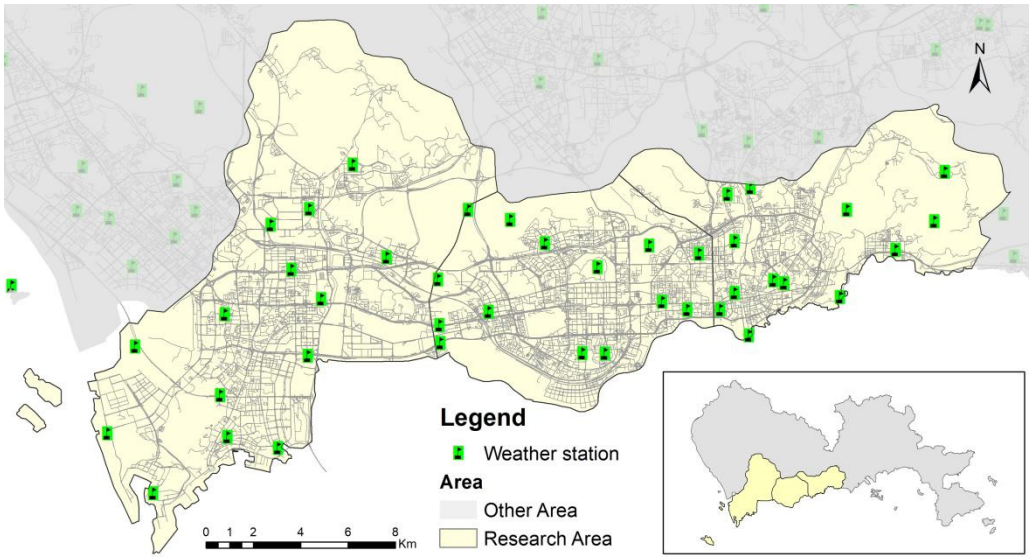


**Figure 1.** Research area.

### 2.2. Dataset

The meteorological data in this study were obtained from the Meteorological Bureau of Shenzhen (https://data.szmb.gov.cn/, (accessed on 4 May 2021). This dataset contains hourly rainfall intensity observed from 44 weather stations from 1 July 2015 to 1 August 2015 (Figure 1). According to the definition of China Meteorological Administration (http://www.cma.gov.cn/, (accessed on 4 May 2021), rainfall of more 8.1 mm/h is considered heavy rain. If the maximum rainfall intensity (during the study period) of a rainy day is more than 8.1 mm/h, it is considered a heavy rain day. Similarly, if the maximum rainfall intensity (during the study period) of a day is 0 mm/h, it is considered a no rain day. Based on the rainfall intensity records, we selected the meteorological data of 10 working days, including 5 heavy rain days and 5 no rain days for the research. The dates and maximum rainfall intensities of heavy rain and no rain days are listed in Table 2. Both heavy rain and no rain days cover Monday to Friday to ensure the representativeness of the sample data.

**Table 2.** The selected rainfall data.

| Heavy Rain Days | | | No Rain Days | | |
|---|---|---|---|---|---|
| **Date** | | **Maximum Rainfall (mm/h)** | **Date** | | **Maximum Rainfall (mm/h)** |
| 24 July 2015 | Friday | 40.25 | 31 July 2015 | Friday | 0 |
| 28 January 2016 | Thursday | 17.20 | 3 November 2015 | Tuesday | 0 |
| 13 April 2016 | Wednesday | 28.02 | 2 December 2015 | Wednesday | 0 |
| 10 May 2016 | Tuesday | 44.35 | 4 February 2016 | Thursday | 0 |
| 6 June 2016 | Monday | 10.28 | 30 May 2016 | Monday | 0 |

With the rapid development of information technology, city-wide data from GPS receivers equipped on taxis have been collected and available. These data have been widely applied in traffic status analyses [19,30,31]. The taxi GPS data used for the travel speed calculations were obtained from the Shenzhen Traffic Operations Command Center, which covers all taxi companies in Shenzhen. The total number of taxis is approximately 15,300. Taxi GPS data include records of the date, time, license plate number, longitude, latitude, instantaneous speed, direction, and taxi status taken every 10 seconds. The dates of the selected taxi GPS data are consistent with the dates in Table 2.

## 3. Methodology

### 3.1. Traffic Speed Calculation

The taxi GPS data were applied to derive the traffic speed of the roads. Because of positioning errors, GPS tracking points seldom match the central line of a road exactly. The first step of calculating the traffic speeds with GPS data was map matching. Since the exact tracks of the taxis were not considered in this study, we used a simple map matching method that can practically handle a large dataset. The transportation network in this study was defined as a directed graph $G(N, A)$, where $N$ is the set of nodes and $A$ is the set of links connecting two nodes. The map matching procedure is described as follows:

(1) For each link $s \in A$, we initiate a point set $M_s = \varnothing$ to store the matched tracking points.

(2) For each GPS tracking point $p$,

(i) search the links nearby within 30 m as candidates $C_p$; and

(ii) then find the fittest link $s$ in $C_p$ using the criterion described as follows:

$$\hat{s} = \begin{cases} \text{argmin } (\Delta\theta_{p,s}), \ if \ \Delta\theta_m < 45^\circ \\ \text{argmin } (d_{p,s}), \ if \ 45^\circ \le \Delta\theta_m < 90^\circ \\ \text{None}, \ if \ \Delta\theta_m \ge 90^\circ \end{cases} \quad (1)$$

where $\Delta\theta_{p,s}$ denotes the difference between the movement direction of the GPS tracking point $p$ and the direction of the link $s$, and $d_{p,s}$ is the distance from $p$ to $s$. $\Delta\theta_m$ is the minimum value of $\Delta\theta_{p,s}$, and it can be calculated as follows:

$$\Delta\theta_m = min\{\Delta\theta_{p,s} | s \in C_p\} \quad (2)$$

(iii) If the fittest link $\hat{s}$ is found in (ii), then append point $p$ to the matched points set $M_{\hat{s}}$ of $\hat{s}$. After map matching, the traffic speed of link $s$ is calculated by the average speed of the GPS tracking points in $M_s$ as follows:

$$v_s = \frac{1}{|M_s|} \sum_{p \in M_s} v_p \quad (3)$$

where $v_p$ is the instantaneous speed of GPS tracking point $p$, and $|M_s|$ is the number of GPS tracking points in $M_s$.

### 3.2. Spatial Interpolation of Rainfall Intensity Data

Rainfall intensity data were usually recorded by weather stations dispersed in the city. In this study, a commonly used spatial interpolation method, the Ordinary Kriging [32], was utilized to obtain the rainfall distribution of the study area. It considers both the distance between weather stations and spatial dependence based on geostatistical analysis.

A schematic diagram of obtaining the rainfall intensity of each road is shown in Figure 2. First, the observed rainfall intensity values from weather stations were interpolated by the Ordinary Kriging for each hour. Then, since roads were represented by their centerlines, we should make a line buffer zone for each road to select the nearby interacted pixels because the rainfall intensity distribution obtained by the Kriging interpolation was a raster image. For each road, the radius of its buffer zone was defined by its width thus that the buffer zone can cover the road. Since few roads were more than 30 m wide (excluding the width of the sidewalk) in the research area, it was reasonable to make a line buffer of 15 m width on each side of a road centerline. Finally, the average value of the pixels in each buffer zone was calculated to represent the road's rainfall intensity.

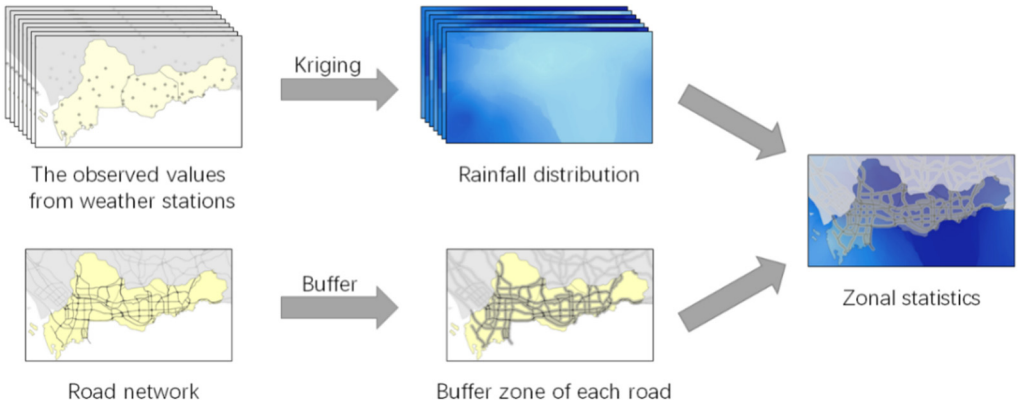


**Figure 2.** The schematic diagram of obtaining the rainfall intensity of each road.

### 3.3. Multistage Model of the Impact of the Heavy Rain Process on Travel Speeds

#### 3.3.1. Heavy Rain Process and Its Stage Division

The rainfall intensity of heavy rain generally increases from zero to the peak and then decreases. Therefore, we propose a multistage model to describe the impact of the various rainfall stages of heavy rain on the travel speeds of links. In this model, a heavy rain event was seen as a process in which the rainfall intensity generally increased from zero to the peak and then decreased. During a time $t = \left[t^{(1)}, t^{(2)}, \ldots, t^{(n)}\right]$, the observed

rainfall intensity of a link $s$ can be represented as $r = \left[r_s{}^{(1)}, r_s{}^{(2)}, \ldots, r_s{}^{(n)}\right]$, and the travel speed on link $s$ during time $t$ is $v_s = \left[v_s{}^{(1)}, v_s{}^{(2)}, \ldots, v_s{}^{(n)}\right]$, where $n$ is the number of time intervals during the heavy rain process. The time interval $\Delta t$ is assumed to be constant and is described as follows:

$$t^{(i+1)} = t^{(i)} + \Delta t, (0 < i < n) \tag{4}$$

An example of a heavy rain process is shown in Figure 3. The horizontal axis, which represents the time $t$, was divided into 3 parts: prepeak, peak, and postpeak. The time $t = t^{(i_0)}$ is when the rainfall intensity reaches the maximum among the three stages and the rainfall intensity of this time $r^{(i_0)}$ is greater than or equal to the threshold $r_0$ ($r_0 = 8.1$ mm/h). Thus, it was considered to be the peak period of heavy rain and named $I_{peak}$. The time $t < t^{(i_0)}$ is the period before the heavy rain peak and is named $I_{pre}$, and the time $t > t^{(i_0)}$ is the period after heavy rain and is named $I_{post}$.

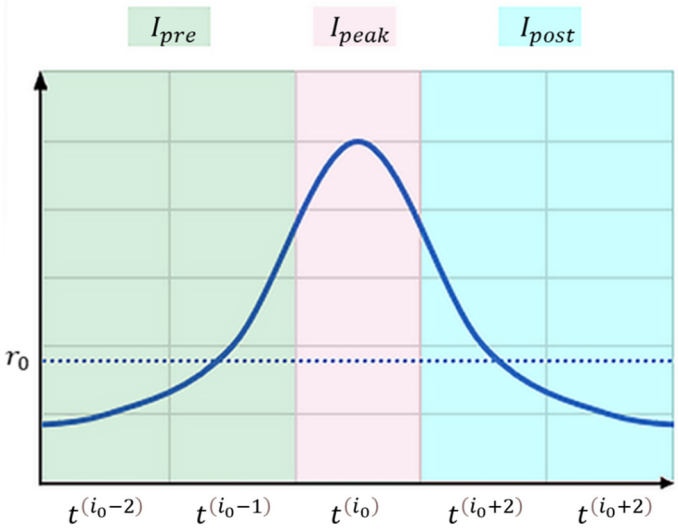


**Figure 3.** Example of the multiple stages of heavy rain.

### 3.3.2. Multistage Impact Model

The difference in travel speeds of links in heavy rain and no rain days was calculated to describe the impacts of heavy rain on urban road traffic efficiency. During a time $t = \left[t^{(1)}, t^{(2)}, \ldots, t^{(n)}\right]$, the speed change ratio (SCR) of a link $s$ is calculated as follows:

$$\Delta v_s = \left(v_{s(r)} - v_{s(c)}\right) \oslash v_{s(c)} \tag{5}$$

where $v_{s(r)}$ and $v_{s(c)}$ are the travel speed vectors of link $s$ in heavy rain and no rain days, respectively. The operator $\oslash$ denotes the pointwise division, which means it divides each vector $\left(v_{s(r)} - v_{s(c)}\right)$ by the corresponding element of the vector $v_{s(c)}$. Thus, an $n$-dimensional vector $\Delta v_s$ represents the impact of heavy rain during each time interval, $\Delta v_s = \left[\Delta v_s{}^{(1)}, \ldots, \Delta v_s{}^{(i)}, \ldots, \Delta v_s{}^{(n)}\right]$.

After the stage division of the heavy rain process, the SCR of link $s$ in the 3 heavy rain stages can be represented by a three-dimensional vector $\left[\Delta v_{s(pre)}, \Delta v_{s(peak)}, \Delta v_{s(post)}\right]$, where $\Delta v_{s(pre)}$, $\Delta v_{s(peak)}$, and $\Delta v_{s(post)}$ are the SCR of link $s$ in the prepeak, peak, and postpeak periods, respectively. These periods can be calculated as follows:

$$\Delta v_{s(pre)} = \frac{1}{|I_{pre}|} \sum_{i \in I_{pre}} \Delta v_s{}^{(i)} \tag{6}$$

$$\Delta v_{s(peak)} = \frac{1}{\left|I_{peak}\right|} \sum_{i \in I_{peak}} \Delta v_s{}^{(i)} \tag{7}$$

$$\Delta v_{s(post)} = \frac{1}{\left|I_{post}\right|} \sum_{i \in I_{post}} \Delta v_s{}^{(i)} \tag{8}$$

The SCR fluctuates greatly for various reasons on different heavy rain days. To reduce the bias when evaluating the trend of the speed change, the median values of $\Delta v_{s(pre)}$, $\Delta v_{s(peak)}$, and $\Delta v_{s(post)}$ on multiple heavy rain days are calculated to describe the general impacts of prepeak, peak, and postpeak heavy rain stages on link $s$, respectively. The impacts can thus be defined as the following SCR vector $x_s$:

$$x_s = [median(\Delta v_{s(pre)}),\ median(\Delta v_{s(peak)}),\ median(\Delta v_{s(post)})] \tag{9}$$

### *3.4. Impact Pattern Discovery Based on the k-Means Clustering Method*

In this study, the patterns of the impact of heavy rain on the traffic speed of links were discovered by the $k$-means clustering method. The method aims to classify all links into $k$ impact patterns. For each link $s$, we can prepare a feature vector $x_s$. Given $m$ links, $m$ feature vectors can be concatenated into a matrix $X = [x_{s_1}, x_{s_2}, \ldots, x_{s_m}]$. The clustering method is described as follows:

(a) Randomly select $k$ samples from $X$ as the initial clustering centers. Then, classify the remaining links based on the similarity measure from the sample clustering centers. The Euclidean norm is used to measure the distance between a road link sample and a cluster center. Assuming $\mu_i$ is the cluster center of the $i^{th}$ cluster $S_i$, $x_s$ is the feature of link $s$. Then, the distance between $x_s$ and $\mu_i$ is:

$$d(x_s, \mu_i) = \parallel x_s - \mu_i \parallel_2 \tag{10}$$

where the $\|\cdot\|_2$ denotes L2 norm of "$\cdot$".

(b) Calculate the center of newly classified links. The new center of $S_i$ can be calculated as follows:

$$\mu_i = \frac{1}{|S_i|} \sum_{s \in S_i} x_s \tag{11}$$

where $|S_i|$ is the number of links in a cluster set $S_i$.

(c) Repeat step (b) until the loss function $J$ has converged.

$$J = \sum_{i=1}^{k} \sum_{s \in S_i} \parallel x_s - \mu_i \parallel_2{}^2 \tag{12}$$

## 4. Experiment and Results

The heavy rain events of the five selected rainy days all occurred in the morning. Figure 4 shows the time distributions of the average rainfall intensity of each rainy day. The figure shows that that the rainfall process of these heavy rain days shows similar prepeak, peak, and postpeak patterns. The duration of the heavy rain peak was shorter than those of the prepeak and postpeak periods. The time distribution of the rainfall intensity was also consistent with the trend of the conceptual model defined in Section 3.3.1.

For the Ordinary Kriging interpolation, the spatial resolution was set as 100 m because of the computational cost. The spherical model was used to describe the semi-variance, and the parameter was fitted by minimizing the deviations to the observed data. The mean absolute error (MAE) and R-square of the interpolation were 1.39 mm and 0.78, respectively, which indicates that the interpolation result was satisfying.

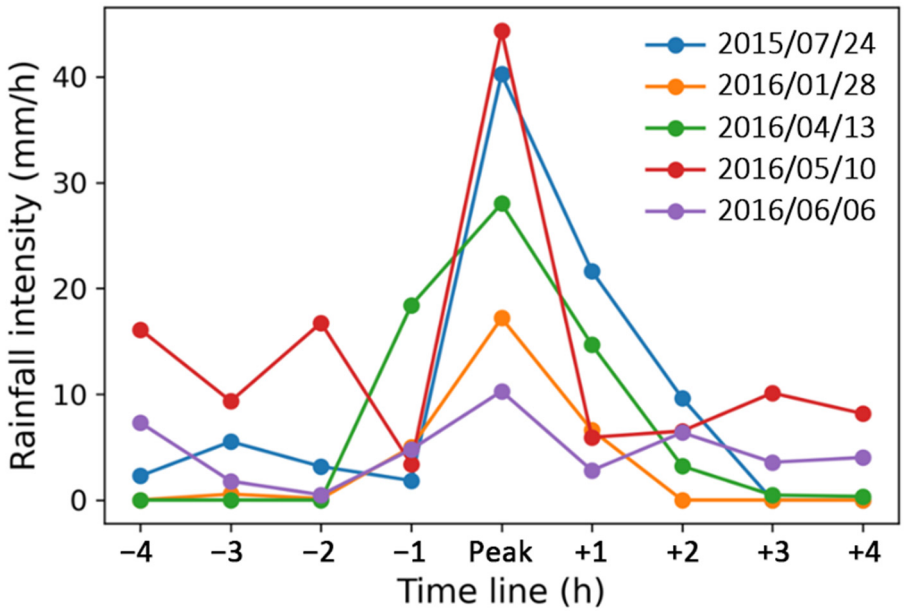


**Figure 4.** Time distribution of the average rainfall intensity on five rainy days.

After the data cleaning procedure, taxi GPS points were matched to the links by the map matching method described in Section 3.1. The average number of GPS tracking points passed on each link in one hour is approximately 100. Then, the average travel speed of each link was calculated using the speed of passing taxis. Since the rainfall data were recorded hourly, the time interval $\Delta t$ in Equation (4) was set as 1 h, and then the average speed of each link was also calculated in hours.

For each link $s$, the SCR vector $x_s$ was calculated using the travel speeds of the links in no rain and heavy rain days, as described in Section 3.4. Then, the k-means clustering method was used to classify the SCR vectors of all links. The sum of squared error (SSE) and Silhouette Coefficient (SC) [33] were used to determine the best $k$. According to the "elbow" rule, the optimal number of clusters should be set as the turning point of the SSE curve. On the other hand, the higher SC represents a better clustering result. As shown in Figure 5, the SSE gradually decreases as $k$ increases from 2 to 10, and the decreasing speed slows down after $k = 3$. Moreover, SC also achieves maximum when $k = 3$. By combing the curves of SSE and SC, it can be found that the best number of clusters is 3. After performing clustering, links in clusters 1, 2, and 3 are 592, 1390, and 457, respectively.

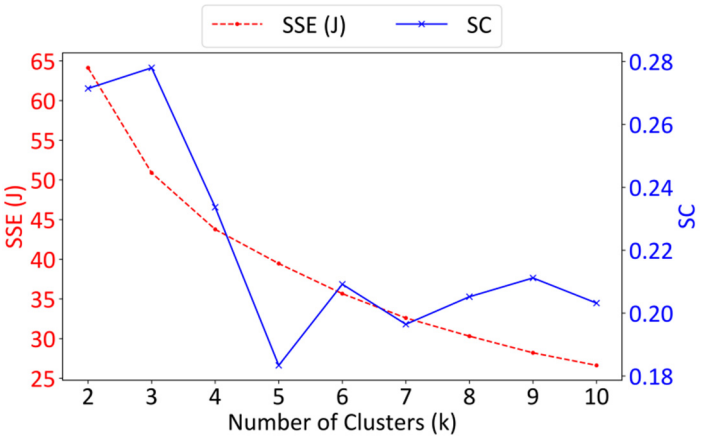


**Figure 5.** The SSEs and SCs with different values of $k$.

The curves of the center of three clusters representing three distinct impact patterns of the heavy rain process on links are shown in Figure 6. The horizontal axis represents three

stages of the heavy rain process, and the vertical axis is the SCR of links at various stages. An SCR greater or less than zero indicates that the travel speed is higher or lower than that on no rain days, respectively. The larger the absolute value of the SCR is, the more significant the speed difference on sunny days. In Figure 6a–c, the translucent polyline represents the curve of vector $x_s$ of a specific link $s$ observed, and the solid black line is the cluster center of each cluster. The upper and lower borders of the colored surface area are the mean value plus and minus the standard deviation, respectively. Figure 6d compares the SCR curves of clusters 1, 2, and 3.

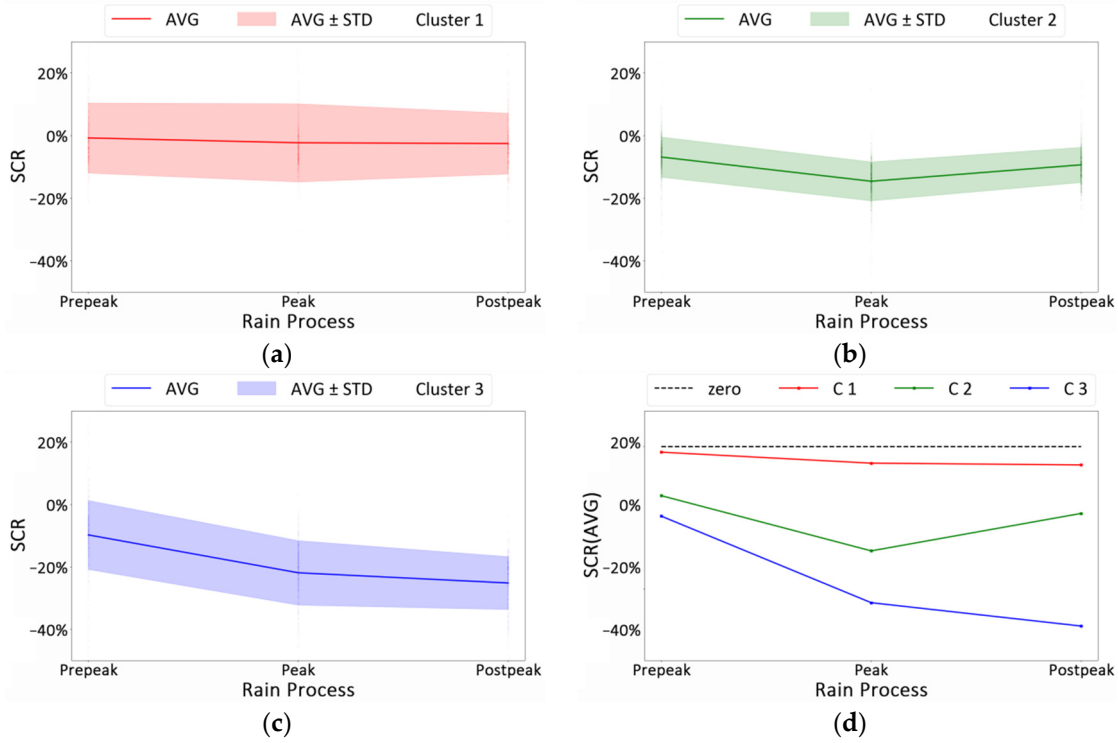


**Figure 6.** The SCR curves of the links of the three clusters during the heavy rain process. (**a**) SCR of cluster 1; (**b**) SCR of cluster 2; (**c**) SCR of cluster 3; (**d**) SCR of three clusters.

As shown in Figure 6, the impacts vary in various heavy rain stages on the links of all three clusters. The impacts are relatively weak in the prepeak stage, whereas the travel speeds of links undergo different extents of decline in the latter two stages because of the cumulative effects of heavy rain. For the links of cluster 1, the travel speeds during the entire heavy rain process are slightly lower than those in no rain days, which means that the impacts of heavy rain on these links are limited, and the cumulative effects of rainfall are also not evident. Among the three clusters, the travel speed deteriorations on cluster 1 were the smallest, and the most significant drop was only 2.6% in the three rainfall stages. Nevertheless, the standard deviations were the largest, indicating that the differences in the SCR among the links of cluster 1 were more significant than those of clusters 2 and 3.

For the links of clusters 2 and 3, the travel speeds during the heavy rain process were much lower than those in no rain days, and they decreased markedly in the peak stage of heavy rain. The difference between clusters 2 and 3 was that the travel speeds of the links of cluster 2 recovered quickly after the heavy rain peak, whereas the traffic speeds of links of cluster 3 droped further in the postpeak stage. Specifically, from the peak to postpeak stage, the speed decline in the links of cluster 2 recovered from 14.65% to 9.39%, but the speed decline in the links of cluster 3 continued to increase from 21.91% to 25.18%. If we do not divide the heavy rain process into consecutive stages, we can only obtain the results that the heavy rain causes a speed decline for these links ranging from 1.93% to 18.95% (Table 3). This finding suggests that when developing traffic management measures

in heavy rain weather, one should focus more on travel speed deteriorations in different rainfall stages. In addition, more attention should be paid to the links of cluster 3 because their speeds are difficult to recover, even if the rainfall intensities decrease again after the heavy rain peak.

**Table 3.** The mean and standard deviation of the SCR of the links of three clusters.

| Clusters | The Mean/Standard Deviation of SCR (%) | | | |
|---|---|---|---|---|
| | Prepeak | Peak | Postpeak | Overall Process |
| 1 | −0.84/11.20 | −2.35/12.46 | −2.60/9.69 | −1.93/7.17 |
| 2 | −6.90/6.41 | −14.65/6.21 | −9.39/5.62 | −10.31/2.86 |
| 3 | −9.77/11.04 | −21.91/10.32 | −25.18/8.46 | −18.95/5.87 |

To test whether the impacts of heavy rain processes on the travel speeds of links are significant, we conducted hypothesis testing on the SCR for three heavy rain stages. The null hypothesis is that heavy rain has no impact on travel speeds, and the mean value of the SCR is equal to zero. The Z-test was used by assuming that SCR follows a normal distribution. As shown in Table 2, the Z-score values of the three clusters are significant under the significance level $\alpha = 0.005$ except for cluster 1 at the prepeak stage, which implies that the heavy rain process has significant impacts on the links in most cases. The Z-score values in Table 4 show that the impacts of heavy rain on the links of cluster 2 are especially significant in the prepeak and peak stages whereas the impacts of heavy rain on the links of cluster 3 are the most significant in the postpeak stage.

**Table 4.** The Z-scores of the links of the three clusters.

| Clusters | Z-Score | | |
|---|---|---|---|
| | Prepeak | Peak | Postpeak |
| 1 | −1.74 | **−4.57** | **−6.49** |
| 2 | **−40.14** | **−87.69** | **−62.27** |
| 3 | **−18.93** | **−45.37** | **−63.60** |

Note: The values in bold represent statistical significance at the 0.005 significance level.

The spatial distribution of links of three clusters is shown in Figure 7a. The red, green, and blue lines are the links of clusters 1, 2, and 3, respectively. The gray lines are not in any cluster because the maximum rainfall intensity on these links is less than the heavy rain threshold (8.1 mm/h), or no taxi GPS data cover these links during the heavy rain events. As shown in Figure 7a, the locations of the links of the three clusters are quite different. The links of cluster 1 are mainly short urban internal roads located at the core of the city, such as the links in and near a street block of Huanggang village shown in Figure 7b. A potential explanation behind this finding is that the travel speeds of these short links are lower than those of other long links. Consequently, the travel speeds are not affected to the same extent. This finding agrees with the research of Tsapakis et al. [5]. The links of cluster 2 are scattered throughout the study area, and they are some short links in the inner part of the city and some long links in the outer part, such as the links in the Futian downtown areas in Figure 7c and Beihuan Avenue in Figure 7d. The links of cluster 3 mainly include some long traffic arteries, such as the G4 Expressway and Xiangmihu Road in Figure 7e.

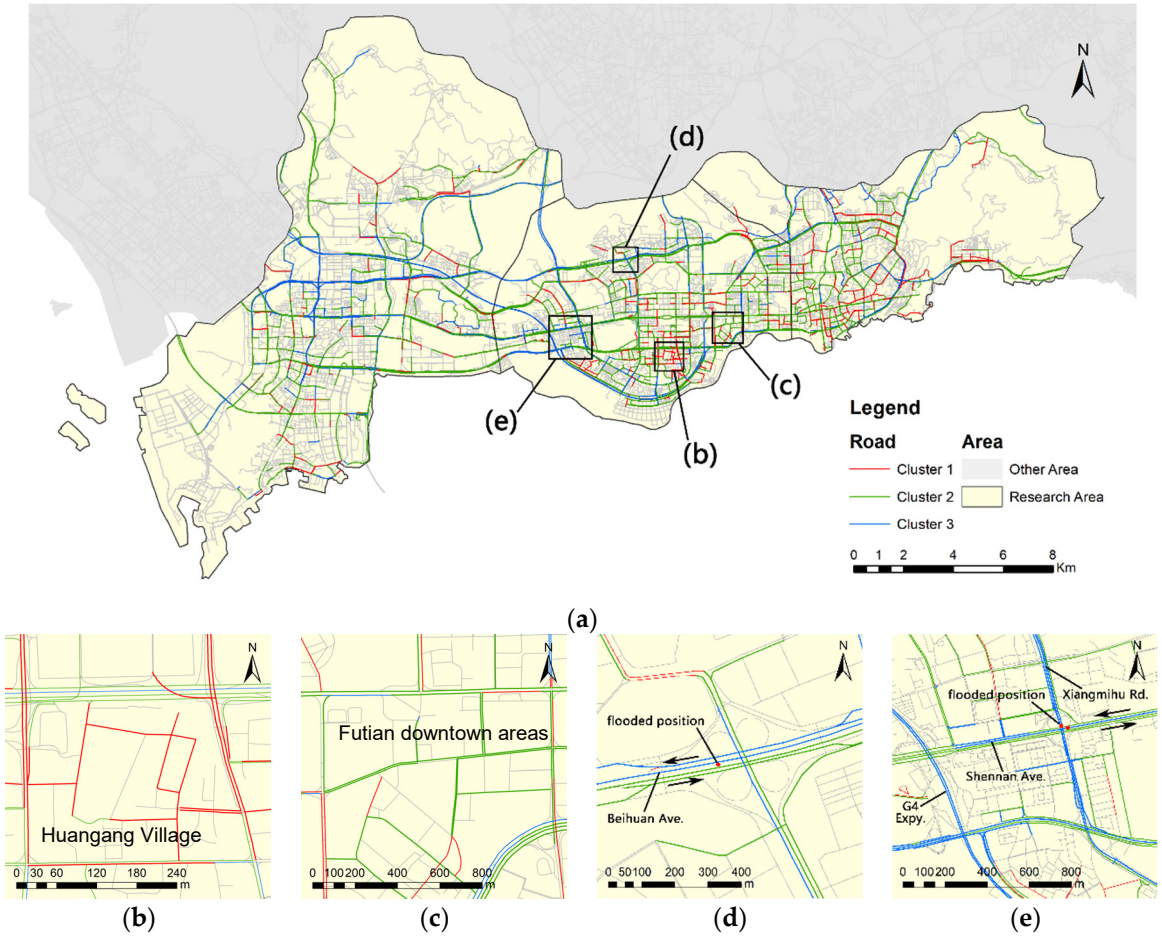


**Figure 7.** The spatial distribution of links of three clusters. (**a**) The spatial distribution of the links of the three clusters; (**b**) links near Huangang Village; (**c**) links in Futian downtown areas; (**d**) Beihuan Avenue is in cluster 2; (**e**) G4 Expressway and Xiangmihu Road are in cluster 3.

Notably, some links belong to different clusters, even if they are in two directions of the same road, such as the links shown in Figure 7d,e. In Figure 7d, Beihuan Avenue from east to west is in cluster 3 while its opposite direction is in cluster 2. In Figure 7e, Shennan Avenue from east to west is in cluster 3 while the segment of its opposite direction (near the crossroad) is in cluster 2. According to the historical information released by the Shenzhen traffic police (https://weibo.com/shenzhenjiaojing, accessed on 4 May 2021), the Beihuan Avenue and Shennan Avenue-Xiangmihu Road crossroads are prone to flooding after heavy rain. The reported flooded positions are shown in Figure 7d,e. Beihuan Avenue from east to the west and Shennan Avenue from east to the west are exactly within the reach of flooded areas. These results suggest that the speed decline in the postpeak stage is probably related to the flooded areas caused by continuous heavy rain and that the accumulated effects of heavy rain are not negligible.

Next, we quantify the differences in the links of the three clusters in the following aspects: road category, travel speeds in no rain days, and the number of transportation facilities (i.e., bus stops and parking lots) along the links. The road category was indicated to be related to the traffic performance of urban roads in rainy weather [20,26,34,35], and we will determine whether it is related to the impact patterns of heavy rain processes. In addition, different road categories represent different expectations of the operational speed under ideal traffic conditions. However, the actual traffic speeds of roads are not always consistent with expectations, especially in rainy weather. Therefore, whether the actual traffic speeds of the links of the three clusters are significantly different is also examined. Furthermore, the transportation facilities along the links have a superimposed effect on

the traffic efficiency of urban roads. For example, bus stops take up road space, resulting in a decrease in road capacity. The entrances and exits of parking lots also have negative impacts on road traffic. We will examine whether the differences in the distribution of bus stops and parking lots along the three clusters of links are significant.

In Figure 8, the proportions of the links with the four different categories in each cluster are calculated. The figure show that more than 70% of links of cluster 1 are CRs or ORs, which are low-grade roads. In contrast, approximately 50% of the links of clusters 2 and 3 are HWUEs or ARs, which are high-grade roads. The proportions of high-grade roads in clusters 2 and 3 are far greater than that in cluster 1.

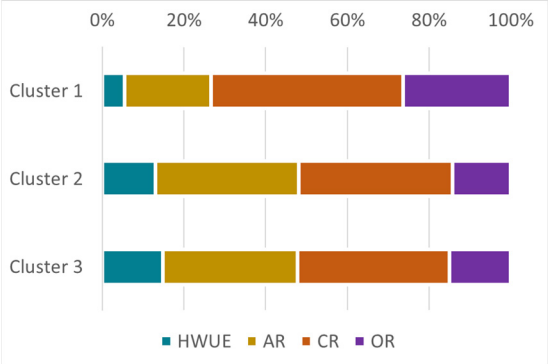


**Figure 8.** The proportions of links in three clusters. (HWUE: highways and urban expressways, AR: arterial roads, CR: collector roads, OR: other roads).

Pearson's chi-squared test was implemented to determine whether the differences in the road category composition of the three clusters were statistically significant. As shown in Table 5, three comparisons except for clusters 2 and 3 were significant at the 0.005 level, which means that the road category composition between clusters 2 and 3 was not significantly different.

**Table 5.** Pearson's chi-squared tests.

| | **Clusters** | | |
|---|---|---|---|
| | **1~2** | **1~3** | **2~3** |
| Pearson's chi-squared | 33.232 | 37.930 | 2.977 |
| Sig. | **0.001** | **0.002** | 0.087 |

Note: The values in bold represent statistical significance at the 0.005 significance level.

The distribution of travel speeds in no rain days and the number of urban transportation facilities (i.e., bus stops and parking lots) along the links are shown in Figure 9. The travel speeds range from interquartile range (IQR) 17.15–29.45 km/h with a median of 22.69 km/h for the links of cluster 1, IQR 20.99–38.59 km/h (median 28.23 km/h) for the links of cluster 2, and IQR 21.52–39.97 km/h (median 29.99 km/h) for the links of cluster 3.

The Kruskal–Wallis (K-W) test was also implemented to test if the indicators of three clusters originated from the same distribution, and the results showed that at least one cluster was significantly (SI $\leq$ 0.001) different from one other cluster in each indicator. Based on the pairwise comparison result, traffic speeds of roads in cluster 1 were significantly lower than that of roads in the other two clusters (SI < 0.001). By combining the SCR curves in Figure 6, it can be found that the heavy rain process had more significant effects on the links with higher traffic speeds in no rain days. Though Figure 8 and Table 5 indicate that roads in clusters 2 and 3 have a similar road category composition, the boxplots of bus stops and parking lots show that the links of cluster 3 are different from those of cluster 2 in transportation facility distribution. The number of bus stops along the links in cluster 2 is significantly larger than that in cluster 3 (SI = 0.001), whereas there is no evidence showing

a significant difference between cluster 1 and the other two clusters. Links in cluster 3 have fewer parking lots than those in cluster 1 (SI = 0.027) and cluster 2 (SI < 0.001).

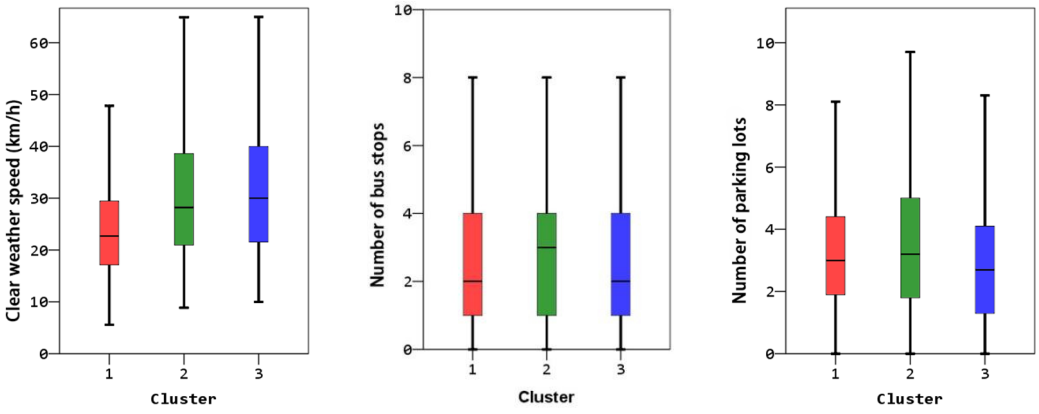


**Figure 9.** Box plots of three indicators. (**a**) Traffic speeds in no rain days; (**b**) bus stops; (**c**) parking lots. Note: The results of the K–W test (K-W Sig.: 0.00 *) show that at least one cluster is significantly different from one other cluster in terms of all indicators (SI $\leq$ 0.001).

## 5. Conclusions

This study investigated the impacts of heavy rain on the traffic speeds of links in different heavy rain stages, i.e., prepeak, peak, and postpeak. An SCR vector was leveraged to represent the speed changes of a link caused by heavy rain in three stages. The *k*-means clustering method was then utilized to cluster the SCR vectors into different groups to find the major impact patterns of the heavy rain process on urban roads. An empirical study of three core districts (i.e., Nanshan, Futian, and Luohu) in Shenzhen, China was conducted to reveal the significant travel speed variation patterns of the links in a real city road network. Finally, the spatial distribution and the characteristics of the links of each cluster are analyzed and compared. This research differs from previous studies by considering the entire rainfall process rather than simply summarizing different rainfall intensity levels.

The findings of the study in Shenzhen suggest that the impacts of heavy rain vary considerably in different stages and on different links. The disparities among the links of the three clusters are distinct. Links of cluster 1 are less affected than those of clusters 2 and 3 at all three stages. For the links of clusters 2 and 3, as the heavy rain process continues, the cumulative effects of rainfall become more evident after the peak stage, and the travel speeds on these links drop rapidly. The difference between clusters 2 and 3 is that the travel speeds of links of cluster 2 recover quickly after the heavy rain peak whereas the travel speeds of links of cluster 3 drop further. By considering three consecutive heavy rain stages, we can observe the impacts of the entire heavy rain process on the travel speed of links, especially the differences in the impacts in the periods before and after the heavy rain peak. This finding suggests that when developing traffic management measures in heavy rain weather, we should focus more on travel speed deteriorations in different rainfall stages. The links of the three clusters are significantly different in their road categories, travel speeds in no rain days, and number of transportation facilities along the links. The findings in this research can contribute to a more in-depth understanding of the relationship between the heavy rain process and travel speeds and provide valuable information for traffic management and personal travel under heavy rain weather. For example, the local government can pay more attention to links with a severe speed decline. For the public, people can choose to avoid those links when planning to travel.

This study has some limitations. First, in our current work, only taxi GPS tracking data were utilized to calculate the travel speeds of urban roads. Because of positioning errors, some GPS points may not be matched to correct roads. As a result, the accuracy of travel speeds on some roads, especially where the GPS positioning error is significant due to signal block or reflection of buildings and trees, can be affected to some extent. If other types of traffic data, such as the data collected from automatic number plate recognition cameras or loop detectors, are available in the future, the travel speeds can be calculated more accurately by fusing them with GPS tracking data. Second, the findings of this study should be further validated with datasets from other areas to determine whether rain effects are region specific. Third, the current study was mainly conducted using data from the morning on weekdays, and further studies should be conducted to investigate the impacts of heavy rain processes on weekends or in other periods of a day. Fourth, the influence mechanism of rainfall on traffic speeds is complicated and comprehensive. Further exploration of the influence mechanism of the heavy rain process on urban road traffic will be implemented in the future.

**Author Contributions:** Qiuping Li: Conceptualization, Data curation, Formal analysis, Methodology, Writing—original draft, Haowen Luo: Methodology, Data curation, Writing—original draft, Xuechen Luan: Data curation, review and editing—original draft. All authors have read and agreed to the published version of the manuscript.

**Funding:** This research was funded by the National Natural Science Foundation of China, grant number 41971345 and the Guangdong Basic and Applied Basic Research Foundation, grant number 2020A1515010695.

**Conflicts of Interest:** The authors declare no conflict of interest.

## References

1. Maze, T.H.; Agarwal, M.; Burchett, G. Whether Weather Matters to Traffic Demand, Traffic Safety, and Traffic Operations and Flow. *Transp. Res. Rec.* **2006**, *1948*, 170–176. [CrossRef]
2. Tam, M.L.; Lam, W.H.; Chen, B.; Chan, K.S.; Wong, S.C. Using automatic vehicle identification data for investigation of rain effects on vehicular travel speeds and travel choice behaviour. In *Traffic and Transportation Studies*; American Society of Civil Engineers: Reston, VA, USA, 2008; pp. 944–955.
3. Koetse, M.J.; Rietveld, P. The Impact of Climate Change and Weather on Transport: An Overview of Empirical Findings. *Transp. Res. Part D Transp. Environ.* **2009**, *14*, 205–221. [CrossRef]
4. Jaroszweski, D.; Chapman, L.; Petts, J. Assessing the Potential Impact of Climate Change on Transportation: The Need for an Interdisciplinary Approach. *J. Transp. Geogr.* **2010**, *18*, 331–335. [CrossRef]
5. Tsapakis, I.; Cheng, T.; Bolbol, A. Impact of Weather Conditions on Macroscopic Urban Travel Times. *J. Transp. Geogr.* **2013**, *28*, 204–211. [CrossRef]
6. Pregnolato, M.; Ford, A.; Wilkinson, S.M.; Dawson, R.J. The Impact of Flooding on Road Transport: A Depth-Disruption Function. *Transp. Res. Part D Transp. Environ.* **2017**, *55*, 67–81. [CrossRef]
7. Ivanović, I.; Jović, J. Sensitivity of Street Network Capacity under the Rain Impact: Case Study of Belgrade. *Transport* **2018**, *33*, 470–477. [CrossRef]
8. Jarmuz, D.; Chmiel, J. A review of approaches to the study of Weather's effect on road traffic parameters. *Transp. Probl.* **2020**, *15*, 241–251. [CrossRef]
9. Chen, P.; Zhang, J.; Jiang, X.; Liu, X.; Bao, Y.; Sun, Y. Scenario Simulation-Based Assessment of Trip Difficulty for Urban Residents under Rainstorm Waterlogging. *Int. J. Environ. Res. Public Health* **2012**, *9*, 2057–2074. [CrossRef] [PubMed]
10. Chen, P.; Zhang, J.; Zhang, L.; Sun, Y. Evaluation of Resident Evacuations in Urban Rainstorm Waterlogging Disasters Based on Scenario Simulation: Daoli District (Harbin, China) as an Example. *Int. J. Environ. Res. Public Health* **2014**, *11*, 9964–9980. [CrossRef]
11. Mitsakis, E.; Stamos, I.; Diakakis, M.; Grau, J.S. Impacts of High-Intensity Storms on Urban Transportation: Applying Traffic Flow Control Methodologies for Quantifying the Effects. *Int. J. Environ. Sci. Technol.* **2014**, *11*, 2145–2154. [CrossRef]
12. Smith, B.L.; Byrne, K.G.; Copperman, R.B.; Hennessy, S.M.; Goodall, N.J. An Investigation into the Impact of Rainfall on Freeway Traffic Flow. In Proceedings of the 83rd annual meeting of the Transportation Research Board, Washington, DC, USA, 11–15 January 2004.
13. Okamoto, N.; Ishida, H.; Furuya, H.; Furukawa, K. Including Weather Condition Factors in the Analysis of the Highway Capacity. In Proceedings of the 83rd annual meeting of the Transportation Research Board, Washington, DC, USA, 11–15 January 2004.
14. Daniel, E. The Mixed Effects of Precipitation on Traffic Crashes. *Accid. Anal. Prev.* **2004**, *36*, 637–647.

15. Agarwal, M.; Maze, T.H.; Souleyrette, R. The Weather and Its Impact on Urban Freeway Traffic Operations. In Proceedings of the 85nd annual meeting of the Transportation Research Board, Washington, DC, USA, 22–26 January 2006.
16. Billot, R.; El Faouzi, N.E.; De Vuyst, F. A multi-level assessment of the rain impact on drivers' behaviors: Standardized methodology and empirical analysis. *Transp. Res. Rec.* **2009**, *2107*, 134–142. [CrossRef]
17. Zeng, W.; Gong, J.; He, Z.; Zhu, Q.; Chen, X. Analysis of Rainfall Impact on Urban Road Traffic Speed. *Environ. Sci. Technol.* **2011**, *34*, 201–205.
18. Lam, W.H.; Tam, M.L.; Cao, X.; Li, X. Modeling the Effects of Rainfall Intensity on Traffic Speed, Flow, and Density Relationships for Urban Roads. *J. Transp. Eng.* **2013**, *139*, 758–770. [CrossRef]
19. Kamga, C.; Yazıcı, M.A. Temporal and Weather Related Variation Patterns of Urban Travel Time: Considerations and Caveats for Value of Travel Time, Value of Variability, and Mode Choice Studies. *Transp. Res. Part C Emerg. Technol.* **2014**, *45*, 4–16. [CrossRef]
20. Zhang, J.; Song, G.; Gong, D.; Gao, Y.; Yu, L.; Guo, J. Analysis of Rainfall Effects on Road Travel Speed in Beijing, China. *IET Intell. Transp. Syst.* **2018**, *12*, 93–102. [CrossRef]
21. Zhang, W.; Li, R.; Shang, P.; Liu, H. Impact Analysis of Rainfall on Traffic Flow Characteristics in Beijing. *Int. J. Intell. Transp. Syst. Res.* **2019**, *17*, 150–160. [CrossRef]
22. Rakha, H.; Farzaneh, M.; Arafeh, M.; Sterzin, E. Inclement Weather Impacts on Freeway Traffic Stream Behavior. *Transp. Res. Rec.* **2008**, *2071*, 8–18. [CrossRef]
23. Zhang, C.B.; Wan, P.; Mei, Z.-H.; Zhang, P.-L. Traffic Flow Characteristics and Models of Freeway under Rain Weather. *J. Wuhan Univ. Technol.* **2013**, *35*, 63–67.
24. Rakha, H.; Arafeh, M. Calibrating Steady-State Traffic Stream and Car-Following Models Using Loop Detector Data. *Transp. Sci.* **2010**, *44*, 151–168. [CrossRef]
25. Wang, L.; Yamamoto, T.; Miwa, T.; Morikawa, T. An Analysis of Effects of Rainfall on Travel Speed at Signalized Surface Road Network Based on Probe Vehicle Data. In Proceedings of the Conference on Traffic and Transportation Studies, ICTTS, Xi'an, China, 2–4 August 2006.
26. Andersen, O.; Torp, K. A Data Model for Determining Weather's Impact on Travel Time. In *Proceedings of the International Conference on Database and Expert Systems Applications*; Springer: Berlin/Heidelberg, Germany, 2016; pp. 437–444.
27. Qi, Y.; Zheng, Z.; Jia, D. Exploring the Spatial-Temporal Relationship between Rainfall and Traffic Flow: A Case Study of Brisbane, Australia. *Sustainability* **2020**, *12*, 5596. [CrossRef]
28. Yao, Y.; Wu, D.; Hong, Y.; Chen, D.; Liang, Z.; Guan, Q.; Liang, X.; Dai, L. Analyzing the Effects of Rainfall on Urban Traffic-Congestion Bottlenecks. *IEEE J. Sel. Top. Appl. Earth Obs. Remote Sens.* **2020**, *13*, 504–512. [CrossRef]
29. Shenzhen Climate Bulletin. 2016. Available online: http://weather.sz.gov.cn/qixiangfuwu/qihoufuwu/qihouguanceyupinggu/nianduqihougongbao/content/post_3578337.html (accessed on 4 May 2021).
30. Zhang, R.; Shu, Y.; Yang, Z.; Cheng, P.; Chen, J. Hybrid Traffic Speed Modeling and Prediction Using Real-World Data. In Proceedings of the 2015 IEEE International Congress on Big Data, New York, NY, USA, 27 June-2 July 2015; pp. 230–237.
31. Li, Q.; Tu, W.; Li, Z. Reliable Rescue Routing Optimization for Urban Emergency Logistics under Travel Time Uncertainty. *Int. J. Geo-Inf.* **2018**, *7*, 77. [CrossRef]
32. Haberlandt, U. Geostatistical Interpolation of Hourly Precipitation from Rain Gauges and Radar for a Large-Scale Extreme Rainfall Event. *J. Hydrol.* **2007**, *332*, 144–157. [CrossRef]
33. Rousseeuw, P.J. Silhouettes: A Graphical Aid to the Interpretation and Validation of Cluster Analysis. *J. Comput. Appl. Math.* **1987**, *20*, 53–65. [CrossRef]
34. Li, Q.; Liu, H.; Zhuo, L.; Tao, H.; Luan, X. Differences in Urban Road Speed Change and Their Influencing Factors during Rainfall. *Trop. Geogr.* **2020**, *40*, 744–751.
35. Yang, C.L.; Sutrisno, H.; Chan, A.S.; Tampubolon, H.; Wibowo, B.S. Identification and analysis of weather-sensitive roads based on smartphone sensor data: A case study in Jakarta. *Sensors* **2021**, *21*, 2405. [CrossRef]